JOTCS B
Journal of the Turkish Chemical Society
Section: B
Chemical Engineering
TURKISH CHEMICAL SOCIETY

Heat Treatment Optimization and Nitriding Effects on Mechanical Properties of 32CrMoV12-10 Steel

Fatih DEMİR[1], Muhammed Bora AKIN[1], Ahmet YARTAŞI[1]*

[1]Çankırı Karatekin University, Department of Chemical Engineering, Çankırı, 18100, Turkiye

Abstract: 32CrMoV12-10 steel is widely utilized in industries where high strength and toughness are crucial. This alloy is commonly used in manufacturing components like gun barrels, gears, and bearings, which demand exceptional mechanical properties. These parts typically undergo heat treatments, including hardening and surface enhancement techniques such as nitriding, to extend their fatigue life significantly. It is crucial to identify optimal heat treatment conditions to achieve desired material performance. In this study, commercial 32CrMoV12-10 steel was selected to investigate the impact of heat treatment parameters (temperature, duration time, and quenching media) on its mechanical properties. To analyse the effect of these parameters, the Technique for Order of Preference by Similarity to Ideal Solution (TOPSIS) and the Taguchi Method were employed, facilitating a systematic examination of the process stages and subsequent mechanical testing outcomes, including Charpy V-notch impact, hardness, and tensile strength assessments. An optimal heat treatment protocol was established based on these analyses, and the nitriding depth of the optimally treated sample was examined using a micro-Vickers hardness tester. For comparative analysis, another sample with closely related outcomes was also evaluated. Results indicated that the surface hardness of the optimally treated Sample 10 reached 870 HV, with a core hardness of 417 HV, compared to non-nitrided Sample 3, which showed a surface hardness of 860 HV and a core hardness of 415 HV. Despite the proximity in their values, Sample 10 exhibited slightly higher micro-Vickers hardness than Sample 3. However, while Sample 3 fails to meet the specified tensile stress and hardness criteria, Sample 10, produced through optimization, meets criteria, ranging from 970 to 1040 N/mm², underscoring the efficacy of the optimization process facilitated by TOPSIS. This optimization was notable for its minimal experimental requirements, proving effective in conserving time, energy, and resources while investigating the processed material.

Keywords: 32CrMoV12-10 steel, TOPSIS based Taguchi Method, Heat treatment, Nitriding, Mechanical properties.

Submitted: December 09, 2023. **Accepted:** June 06, 2024.

Cite this: Demir, F., Akın, Muhammed B., & Yartaşı, A. (2024). An Investigation into Different Heat Treatment Conditions on Mechanical Properties and Nitriding of 32CrMoV12-10 Steel. Journal of the Turkish Chemical Society, Section B: Chemical Engineering, 7(2), 121–138. https://doi.org/10.58692/jotcsb.1402484.

***Corresponding author. E-mail:** mbakin@karatekin.edu.tr.

1. INTRODUCTION

The application of various coatings (such as laser, chrome, etc.), production methods, and heat treatment techniques holds significant importance in conferring specific properties to steel materials. These processes aim to enhance the material's resistance to both corrosion and abrasion (Saklakoğlu et al., 2016). It has been reported that the parameters of the heat treatment process and the chosen production methods significantly impact the material's behavior during manufacturing, influencing surface hardness and tension, regardless of whether machining is involved or not (Toktaş et al., 2017).

Advancements in weapon technology have observed significant progress. Throughout this developmental journey, a marked improvement has been witnessed in achieving high strength, toughness, enhanced wear resistance, and superior corrosion resistance. Consequently, gun barrels have become lighter and

have demonstrated superior properties concerning abrasion (GÖKSU, 2015).

Presently, the global arms market specifies an increase in the expected firing life for light, medium, and high-caliber barrels compared to standard requirements. The barrel's shot life, varying by caliber, stands at 50,000 shots for light weapons. However, this number decreases as the caliber size increases due to heightened pressure. Material composition, heat treatment methods, and coating types significantly influence the firing life of weapons (Rutci, 2019).

Research indicates that firearms experience high pressures and temperatures during operation. Upon the ammunition core's exit from the barrel, a considerable increase in temperature and pressure occurs in the barrel chamber. This phenomenon stems from the pressure exerted by gunpowder against the barrel walls, along with a rapid temperature surge within the barrel steel, leading to material stress. Therefore, the selection of materials should prioritize strength, durability, and high impact resistance to ensure extended life with superior dimensional stability (Karslı et al., 2021).

A study examining the effect of heat treatments on the mechanical properties of 42CrMo4, a steel known to be more expensive than 36CrB4, revealed that by adjusting the tempering temperature of 36CrM4 steel, similar mechanical properties to 42CrMo4 steel could be achieved, leading to cost savings (Karslı et al., 2021).

Furthermore, in another study, XRD (X-Ray Diffraction) results and hardness evaluations of X40CrMoV51 high alloy steel were conducted following ion nitriding post-tempering and quenching. The study noted that the nitrided surface exhibited twice the hardness compared to the quenched surface. The study highlighted that in applications where hardness is crucial, the material's high resistance to corrosion and wear significantly contributes to increased lifespan (Karslı et al., 2021).

Gas nitriding applied to 32CrMoV12-10 steel has been observed to provide a surface hardness at least 1.5 times higher than that achieved through quenching and tempering processes (Karslı et al., 2021).

Studies applying gas, plasma, and solid nitriding to AISI H13, N-8550, and AISI P20 steels reported an increase in surface hardness for these steels (Almeida et al., 2015).

In a separate study, plasma nitriding was performed on AISI 420, 416, 410NiMo, and 410 martensitic stainless steels at various temperatures, leading to an enhancement in the surface hardness of the martensitic stainless steels. However, an exception was noted in the form of a reduced surface hardness, attributed to the precipitation of Cr alloy and CrN, which binds nitrogen. This was in contrast to the results at 450 °C, with the exception being the 410NiMo steel at 500 °C, where no decrease in hardness was observed (Ferreira et al., 2015).

Furthermore, it was found that the application of gas nitriding to DIN1.2344 hot work tool steel resulted in improved wear resistance (Bakdemir et al., 2020). To improve efficiency in the production process by reducing time, costs, and waste, the effectiveness of materials whether they pass or fail the quality control tests during nitriding is assessed (Perraki & Orfanoudaki, 2004; Roussel et al., 2010; Scholte et al., 1984).

The literature review highlights numerous studies focusing on the hardening of steels using diverse processes and methodologies. Nonetheless, there is a noticeable absence of research employing the TOPSIS-based Taguchi Method for optimizing the heat treatment process specifically aimed at hardening 32CrMoV12-10 steel. This study, therefore, addresses a significant gap in the current body of knowledge. In our approach, a three-factor, three-level experimental design was applied to 32CrMoV12-10 steel, which is typically supplied in either rolled or forged conditions for subsequent machining and forming operations. The decision to undertake machining on machine tools for this steel type was guided by the insights gained through the application of the TOPSIS-based Taguchi Method. This methodological choice aims to enhance the efficiency of the production process by reducing time, costs, and material waste, while also considering the outcomes of quality control checks, particularly focusing on the steel's performance post-nitriding treatment.

In this context, our study includes the application of various heat treatment regimes to 32CrMoV12-10 steel using the Taguchi method and subsequently evaluates the resulting mechanical properties to identify the most effective heat treatment conditions. The investigation extended to examining the influence of nitriding on steel exhibiting optimal mechanical strength characteristics. The findings suggest that the proposed optimization process not only fills a crucial gap in the literature but also demonstrates that significant process improvements are achievable with relative ease by adopting the suggested method.

2. EXPERIMENTAL SECTION

2.1. Materials

In this study, 32CrMoV12-10 steel suitable for hardening and tempering will be used. The chemical component analysis of 32CrMoV12-10 steel is given in Table 1 (SIJ GROUP 2020).

Table 1: Chemical analysis of 32CrMoV12-10 Steel (% wt.).

Chemical Compound	% Component
C	0.32
Cr	3
Mo	1
V	0.30
Si	Max. 0.35
Mn	Max. 0.60

Three cylindrical specimens of 32CrMoV12-10 steel, each measuring 100 mm x 70 mm (height x radius), were supplied for the experiments. These specimens were cut with a minimum wall thickness of 15 mm using a saw, as illustrated in Figure 1. Additionally, each specimen was assigned a unique identification number.

After conducting the tensile, Charpy impact, and hardness measurement tests, the samples were subjected to the nitriding process. This process was determined based on two test conditions, one yielding the best results and the other the worst, within the desired value range according to the Taguchi Method. The nitriding capacity of the material and the depth of nitrogen penetration under two distinct test conditions were assessed and compared.

2.2. Sample Preparation and Testing for Heat Treatment

The steel test specimens, all with identical wall thicknesses for heat treatment, were cut into nine separate pieces measuring 12x12 cm². Figure 2 illustrates the specimens sliced into plates.

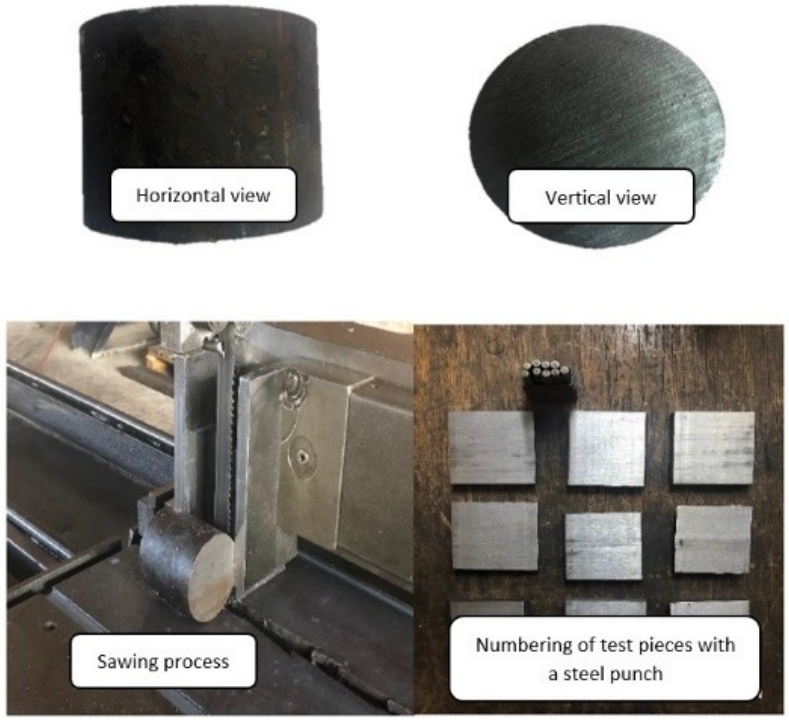

Figure 1: Preparation of 32CrMoV12-10 steel for heat treatment.

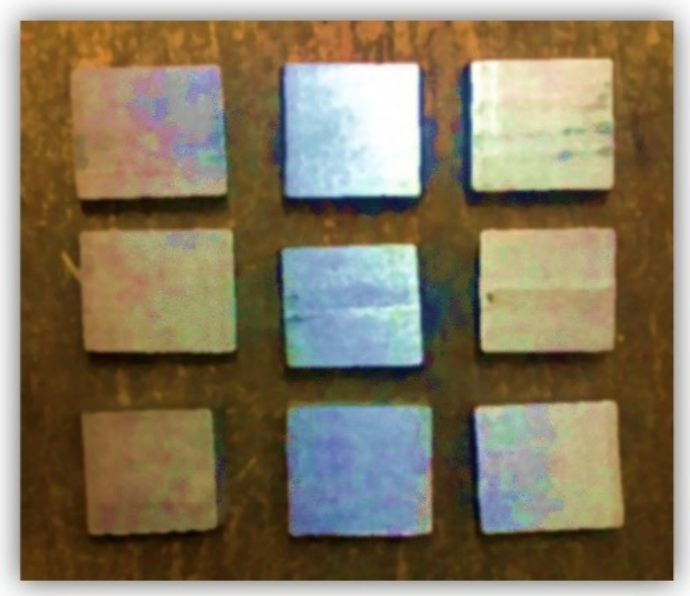

Figure 2: 32CrMoV12-10 steel specimens with equal wall thicknesses sliced and ready for heat treatment.

In determining the heat treatment parameters for commercial 32CrMoV12-10 steel, the decision was made based on the region where the highest impact notch value was observed, which was derived from the literature and technical documents provided by the manufacturer. The identification of the temperature and time parameters was guided by the temperature-time graphs provided for characteristic hardening. Similarly, the selection of the quenching media was informed by the literature and technical documentation from the manufacturer (ARMAD, Tekin).

The experimental design followed the Taguchi L_9 Method, utilizing predefined factors and levels as outlined in Table 2. Table 3 details the experimental setup comprising three controllable variables (Factor A, Factor B, and Factor C) with three corresponding levels for each factor (Level 1, Level 2, and Level 3).

Table 2: The factors selected for the experimental design and their level values.

Factors	**Level 1**	**Level 2**	**Level 3**
A- Temperature (°C)	925	950	975
B- Duration Time (min)	45	60	75
C- Quenching Media	Water	Heat Treatment Oil	10% salt water

The graphs depicting the heat treatment process applied to the specimens are presented in Figure 3. In this graph, the initial stage involves preheating, intended to mitigate abrupt cooling effects, enhancing temperature penetration within the material and facilitating the formation of a more ductile grain structure, namely pearlitic, within the heat-affected zone. Subsequently, the material is heated to the specified treatment temperature, and once the specimens reach the austenitizing temperature, they are quenched after a defined time interval to harden the material.

Table 3: Experimental setup determined by the L9 orthogonal array.

Exp. No	Factors A	B	C
1	1	1	1
2	1	2	2
3	1	3	3
4	2	1	2
5	2	2	3
6	2	3	1
7	3	1	3
8	3	2	1
9	3	3	2

The heat treatment process is initiated within the retort, depicted in Figure 4, adhering to the assigned variables and levels according to the L9 orthogonal sequence. Following the preheating ramp of the furnace temperature and stabilization at the set soak temperature for a specific duration, the specimens undergo the hardening process as they are transferred into the quenching media.

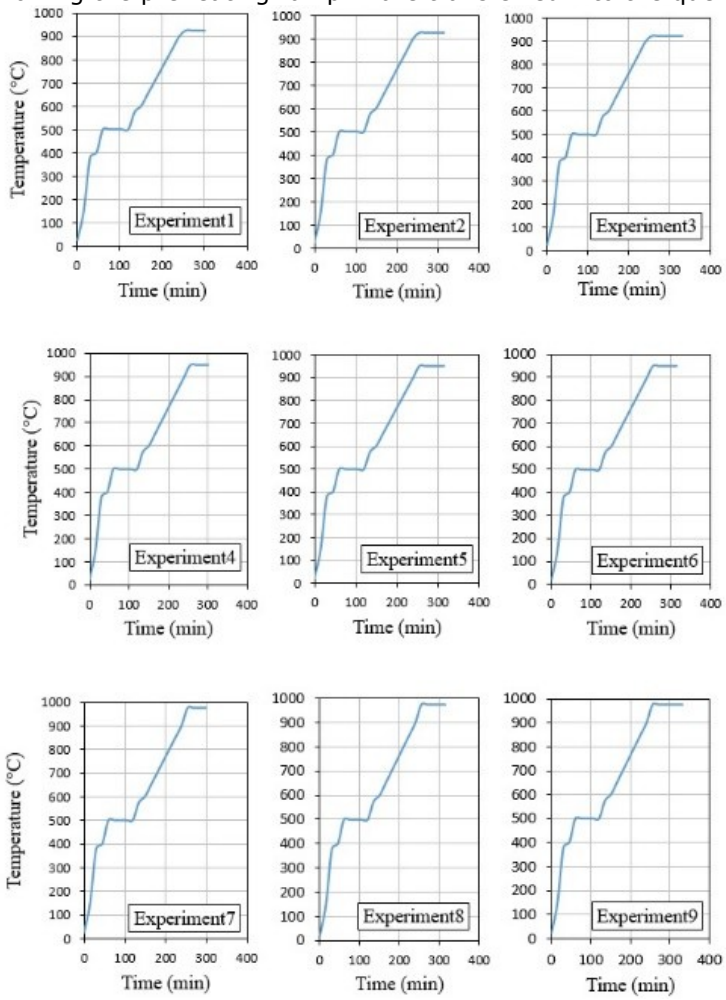

Figure 3: Heat treatment program applied for the specimens in the experiments.

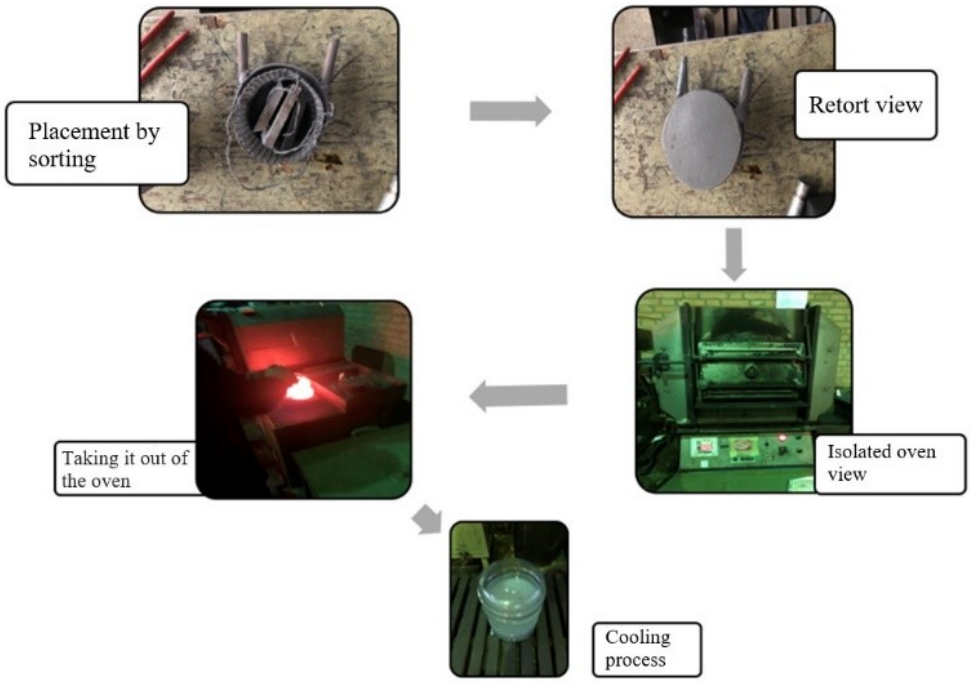

Figure 4: Heat treatment and quenching stages in the experimental.

As depicted in Figure 3, the heat treatment procedure extends up to a maximum duration of 330 minutes. Subsequent to the quenching process, illustrated in Figure 4, the specimens undergo tempering (held at 550 °C for 300 minutes) with the aim of enhancing material toughness.

The heat-treated specimens, illustrated in Figure 5a, were subjected to blasting using S170 steel shot to prepare them for entry into the testing environment, as shown in Figure 5b. This sandblasting process effectively removes surface oil, rust, and metal residue, thereby ensuring the surface of the material is suitably prepared for laboratory conditions.

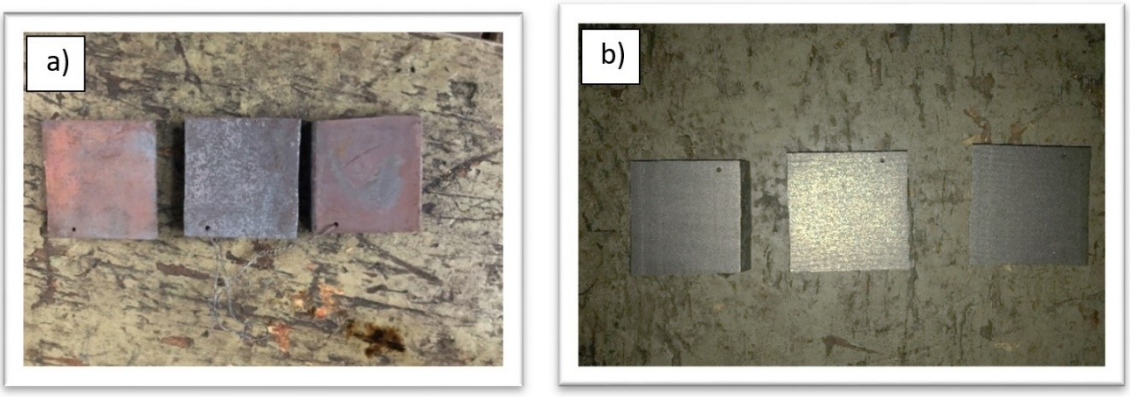

Figure 5: (a) Crusted surface after heat treatment and (b) surface after blasting (S170).

2.2.1. Specimen preparation for Charpy impact V-notch test

After the heat treatment process, materials measuring 12x100 mm were processed using a milling machine to create Charpy impact test specimens following the guidelines outlined in the ISO 148-1 standard (Figure 6). Subsequently, the notches were precisely formed on the milling machine, rendering the material ready for testing.

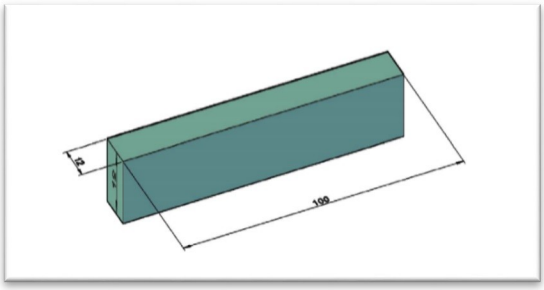

Figure 6: Schematic representation of specimen conforming to ISO 148-1 standard for Charpy impact V-notch test.

For the Charpy impact V-notch test, a notch, 9 mm wide and 2 mm deep, was created at the center of each specimen, conforming to the specifications defined in the ISO 148-1 standard.

2.2.2. Application of the Charpy impact V-notch test

The Charpy impact test aims to measure the energy, recorded in joules, at the moment of initial impact when breaking a test piece. This is achieved by using a hammer capable of circular motion within a protective enclosure, as depicted in the schematic diagram in Figure 7a.

The Charpy impact tester, illustrated in Figure 7b, comprises an internal mechanism with a hammer moving in circular motion, a mechanism to hold the hammer in place, an anvil to position the specimen, and an outer casing encompassing the entire system with wire mesh to safeguard the specimen from potential splintering or damage due to the impact of the hammer.

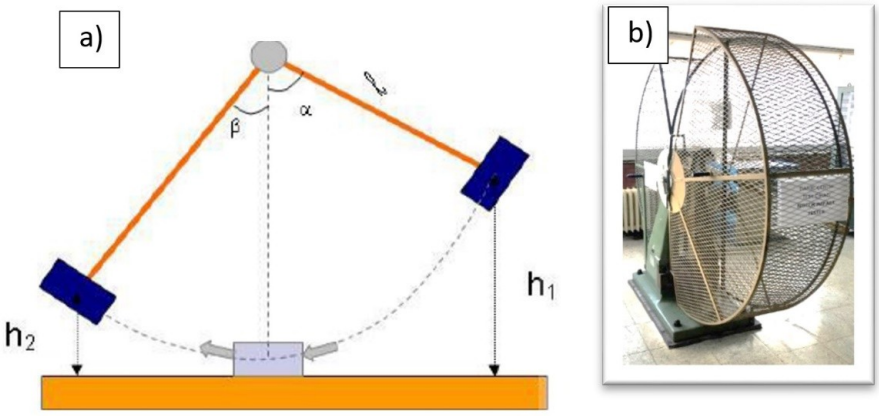

Figure 7: (a) Schematic illustration displaying the internal mechanisms of the Charpy impact tester, and outlining the operational principles of the device, and (b) Charpy impact test device.

In the Charpy impact test following the ISO 148-1 standard, the test specimen is placed on the anvil with the notch facing inward. Upon releasing the hammer from a specific height "h" behind the V-notch, the specimens, positioned both vertically and horizontally, assume their final orientation. Figure 8 illustrates the functionality of the impact notch test mechanism and the resulting specimens from the experiment.

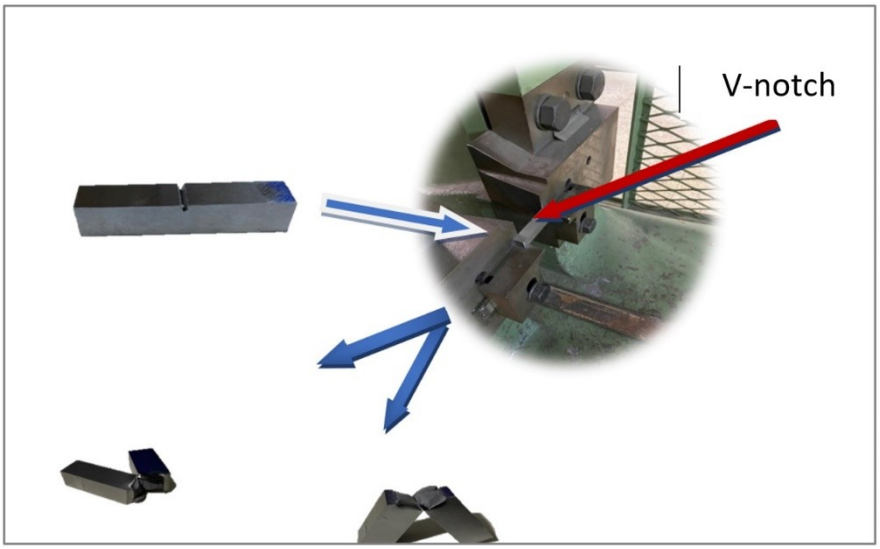

Figure 8: Images of the specimens before and after undergoing the Charpy impact test.

2.2.3. Tensile test specimen preparation
After undergoing heat treatment, the specimens were machined using a universal lathe in compliance with the TS EN ISO 10002-1 standard to prepare them for the tensile test. M10 threads were drilled on both ends of the specimens using the lathe. The dimensions of the specimens are illustrated in Figure 9.

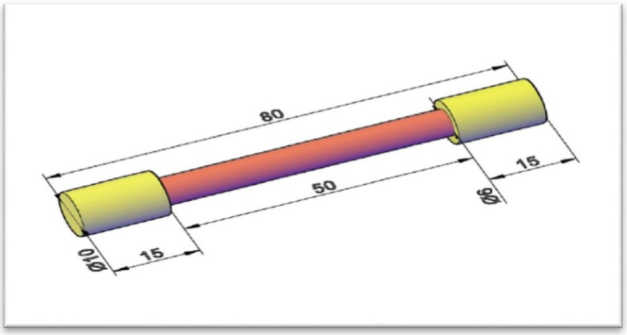

Figure 9: Dimensions of the tensile test bar specimen in millimeters along with a schematic representation.

2.2.4. Tensile Test Procedure
The 20-ton Galdabini brand tensile testing machine was utilized to measure the yield strength, ultimate tensile strength, and percentage of elongation of the samples. The specimen is affixed to the tester's jaws in accordance with the drilled thread diameter for the part under examination. The tester applies an incremental upward and downward force "F" to the fixed portion. The maximum tensile force is derived from the resulting graph plotted by the tensile tester, correlating "F" force with plastic deformation.

Figure 10 displays the tensile test bar connected between the two jaws, emphasizing the region denoted by the red ellipse indicating a specific elongation, signifying the material's transition into plastic deformation. Additionally, the figure illustrates the outcome of the tensile test leading to the rupture of this material.

2.2.5. Brinell Hardness Testing Procedure
The measurements were conducted using a Wolpert brand hardness tester, and the results were evaluated and recorded in duplicate reports.

Hardness measurements were carried out in the laboratory environment using the Wolpert device. The process involved placing the material on the lower table and applying pressure to crush the material by releasing the load. The hardness result was determined by manually measuring the diameter of the impression with the aid of a ruler and under proper lighting conditions.

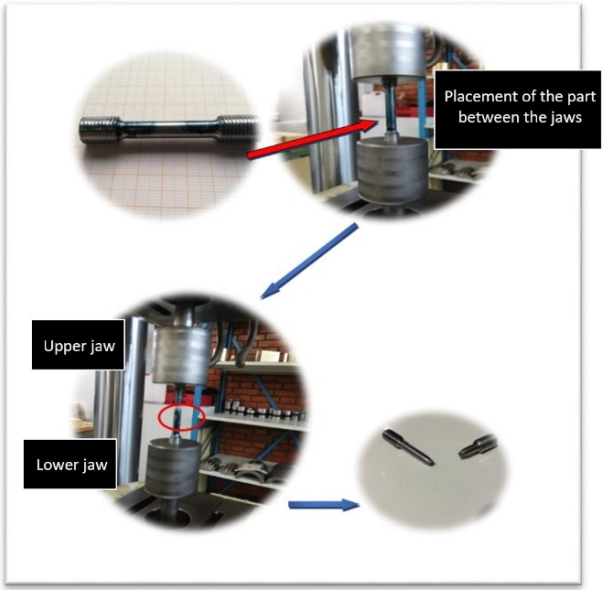

Figure 10: Images of the tensile test specimen: before and after testing.

2.2.6. Microhardness Measurements

For the microhardness measurements, the samples were encased in bakelite and compressed, as depicted in Figure 11a. Subsequently, they underwent a polishing process, as shown in Figure 11b.

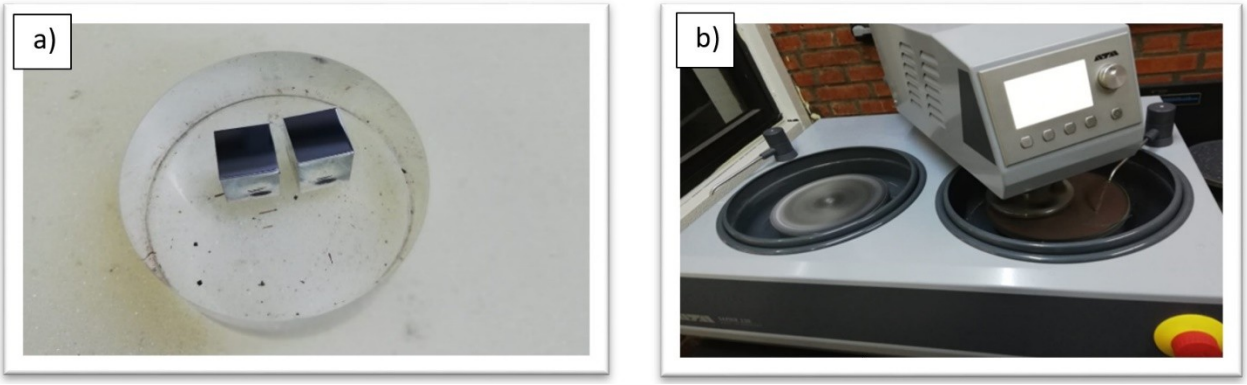

Figure 11: (a) Samples taken on bakelite, and (b) surface cleaning of samples before analysis.

Using the Ness brand device, the nitration penetration and core hardness of the samples within the prepared bakelites were measured. The results regarding nitrogen diffusion were obtained from the software integrated with the device.

Following the calibration of the Ness brand microhardness analyser, the samples were positioned. Upon activation of the device, the lenses detected the positions, and data were collected after approximately 20 minutes of scanning, employing 100x and 1000x magnification for measuring the initial trace and subsequently the opened trace.

2.3. Calculations for TOPSIS method

In the study, responses obtained through the Taguchi method are processed, and the TOPSIS (Technique for Order Preference by Similarity to the Ideal Solution) method is applied. Naturally, the targeted values are intended to be optimized either to their minimum or maximum levels. Through the TOPSIS method, values aimed at minimization are brought to the lowest possible level, and those aimed at maximization are elevated to the highest possible level. This process thus simplifies reaching the most ideal solution in terms of proximity. After forming the decision matrix, it is necessary to normalize the target values and determine their weights to obtain standardized measurement units (Hwang and Yoon, 1981).

The initial step in the TOPSIS calculation of the study is to use the responses derived from the Taguchi method to create a standard decision matrix. This standard decision matrix is generally expressed as Equation 1, and with the utilization of the results, the standard decision matrix as outlined in Equation 2 is obtained.

$$R_{ij}=\frac{a_{ij}}{\sqrt{\sum_{k=1}^{m} a_{kj}^2}} \quad (1)$$

$$R_{ij}=\begin{bmatrix} r_{11} & r_{12} & \dots & r_{1n} \\ r_{21} & r_{22} & \dots & r_{2n} \\ \cdot & \cdot & \cdot & \cdot \\ \cdot & \cdot & \cdot & \cdot \\ \cdot & \cdot & \cdot & \cdot \\ r_{m1} & r_{m2} & \dots & r_{mn} \end{bmatrix} \quad (2)$$

The formation of the weighted standard decision matrix constitutes the initial step. In the calculations, the total of the weighted values for the evaluation criteria is determined as illustrated in Equation 3 (Şimşek, 2014).

$$\sum_{i=1}^{n} w_i=1 \quad (3)$$

Following the establishment of the weighted standard decision matrix, the next step involves multiplying each value in the columns of the standard decision matrix by the corresponding weight value (w_i) to construct the weighted standard decision matrix as demonstrated in Equation 4 (Şimşek, 2014).

$$V_{ij}=\begin{bmatrix} w_1 r_{11} & w_2 r_{12} & \dots & w_{11} r_{1n} \\ w_1 r_{21} & w_2 r_{22} & \dots & w_n r_{2n} \\ \cdot & \cdot & \cdot & \cdot \\ \cdot & \cdot & \cdot & \cdot \\ \cdot & \cdot & \cdot & \cdot \\ w_1 r_{m1} & w_2 r_{m2} & \dots & w_n r_{mn} \end{bmatrix} \quad (4)$$

Subsequently, the formation of the ideal (A^*) and the negative ideal (A^-) solutions is undertaken. To generate the ideal solution set, the largest values for the standardized criteria within the weighted standard decision matrix are selected. The formula for constructing the positive ideal solution set is given in Equation 5.

$$A^* = {}^{max}_{i} V_{ij} \,\middle|\, j \epsilon J \;\; {}^{min}_{i} V_{ij} \,\middle|\, j \epsilon J' \quad (5)$$

Through Equation 5, the calculated set is expressed as $A^* = \{v_1^*, v_2^*, \dots, v_n^*\}$.

Conversely, when identifying the negative ideal solution set, the smallest values for the normalized criteria within the weighted standard decision matrix are chosen. The equation used to find the negative ideal solution set is presented in Equation 6 (Şimşek 2014).

$$A^- = \text{❑} \vee \text{❑} \; {}^{min}_{i} V_{ij} \,\middle|\, j \epsilon J \;\; {}^{max}_{i} V_{ij} \,\middle|\, j \epsilon J' \quad (6)$$

Using Equation 6, the set calculated is expressed as $A^- = \{v_1^-, v_2^-, \dots, v_n^-\}$.

In both equations, the two expressions represent J as the benefit (goal is maximum) and J' as the cost (goal is minimum) values. It is observed that either the positive or negative ideal solution set consists of n elements, corresponding to the number of evaluation factors.

Upon reaching the Calculation of Separation Measures step, determining the deviations from the ideal and negative ideal solution sets necessitates establishing the deviation values for the decision points. These values emerge as the positive ideal separation and negative ideal separation, respectively denoted as Equation 7 and Equation 8 (Şimşek 2014).

$$S_i^* = \sqrt{\sum_{j=1}^{n} \left(v_{ij} - v_j^*\right)^2} \quad (7)$$

$$S_i^- = \sqrt{\sum_{j=1}^{n} \left(v_{ij} - v_j^-\right)^2} \quad (8)$$

The numbers S_i^* and S_i^- to be calculated will be as many as the response numbers in the experimental design (Şimşek 2014).

In the final step, calculating the distance of the decision points from the ideal solution utilizes S_i^* and S_i^-values. The relative closeness to the ideal solution is the ratio of the S_i^- value to the sum of the S_i^* and S_i^-values (Equation 9) (Şimşek 2014).

$$C_i^* = \frac{S_i^-}{S_i^- + S_i^*} \quad (9)$$

Values calculated with Equation 9 will naturally range between 0 and 1 ($0 \leq C_i^* \leq 1$). When considered independently, the highest C_i^* value is selected. However, in the TOPSIS-based Taguchi method, C_i^* values are further assessed using the Taguchi method, thereby achieving the final optimization results.

2.4. Nitriding process

Following the optimization of the heat treatment process with the Taguchi method, Sample 10 was produced. Subsequently, Sample 10 underwent a nitriding process. Gas nitriding was applied for 72 hours at 540 °C. After nitriding, comparisons were made between Sample 3, which had the best test results, and the nitrided Sample 10.

3. RESULTS AND DISCUSSION

The experimental design was completed using the levels automatically assigned to the factors in the L9 orthogonal array. The duplicate results from the tensile strength, impact notch, and hardness tests are presented in Table 4. The experimental data were processed utilizing the Taguchi Method within the Minitab program.

Table 4: According to the L_9 Taguchi Method, the results of the experiment.

Exp. No	Tensile Strength* (N/mm²)		Impact Notch** (J)		Hardness* (N/mm²)	
1	874	877	181	178	930	965
2	940	945	180	175	965	995
3	1049	1035	133	138	1125	1120
4	929	935	180	177	965	962
5	976	983	150	149	1060	1045
6	1135	1129	124	127	1190	1155
7	1137	1142	124	123	1118	1155
8	997	986	153	150	1060	1045
9	1003	989	156	159	1060	1048

* It is desired to be in the range of 970-1040 N/mm²
**It is desired to be greater than 40 J.

3.1. Optimizing Material Testing Outcomes Using Taguchi Method and TOPSIS Analysis

The analysis of duplicate results from the tensile test, impact notch test, and hardness measurement experiment was conducted following the Taguchi Method, employing both the "larger is better" and "nominal is best" criteria as applicable. This method was chosen to identify the highest achievable values considering various factors (Factor A, Factor B, and Factor C) and their levels (Level 1, Level 2, Level 3) across the experiments. In the figures corresponding to each test (Figures 12, 13, and 14), factors are illustrated with green circles, levels with yellow circles, and the optimal values targeted are marked with red circles. The objective was to pinpoint the maximum value achievable based on the defined factors and levels for each type of test. The Minitab software package was utilized to document the outcomes of these analyses. The insights from the data points, particularly those underscored by the red circles in the figures, were harnessed to synthesize the dataset into a singular result using the TOPSIS method, thereby streamlining the analysis process and enhancing the efficiency of identifying optimal conditions across different types of material tests.

Figure 12: "Larger is better" recommendation for tensile experiment according to Taguchi Method.

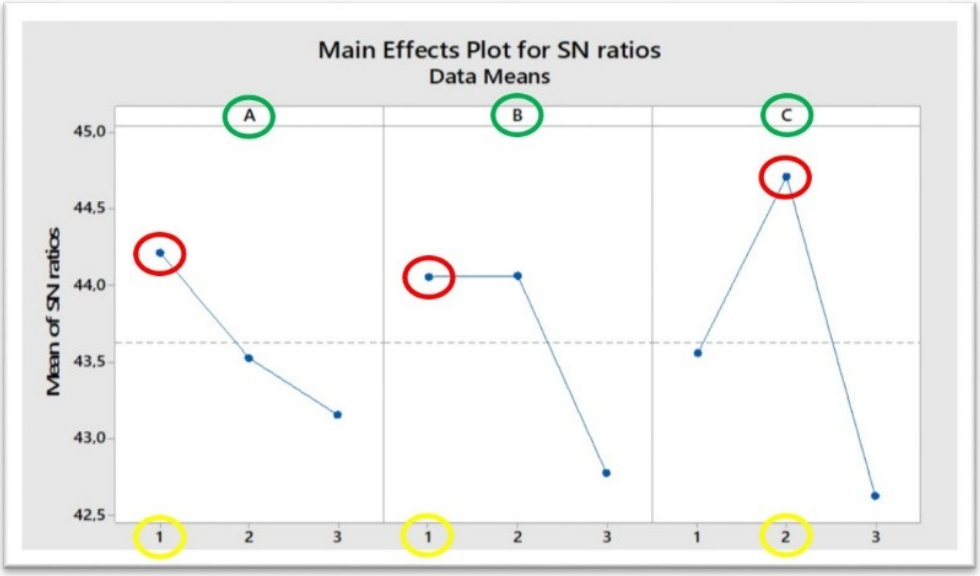

Figure 13: S/N ratios of impact notch test according to Taguchi Method.

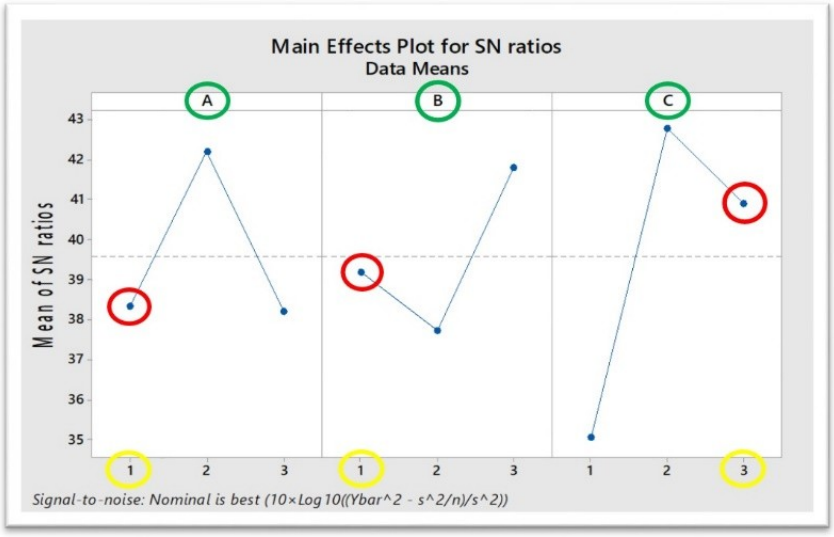

Figure 14: S/N ratios of hardness test according to Taguchi Method.

3.2. TOPSIS Based Taguchi Method Results

The replicated results of the tensile, V-notch, and hardness measurement tests underwent analysis using the variable of "nominal is better" or "larger is better" according to the Taguchi method, as illustrated in Figure 12, Figure 13, and Figure 14. The distribution variation of three factors across different levels was examined. As the values highlighted with the red circle influence strength, fracture, and toughness interdependently, optimal values were selected for the best experimental design utilizing the TOPSIS method.

The data obtained after the application of the Taguchi and TOPSIS methods and the duplicate results closest to the optimum desired values are shown in Table 5.

The data derived from the TOPSIS method were subsequently integrated back into the Taguchi Method, employing the "larger is better" approach to enhance strength and toughness within the experimental design, and an analysis was conducted. In the results depicted in Figure 15, green circles indicate the factors, yellow circles represent the levels, and red circles signify the maximum values to be attained based on the factors and levels.

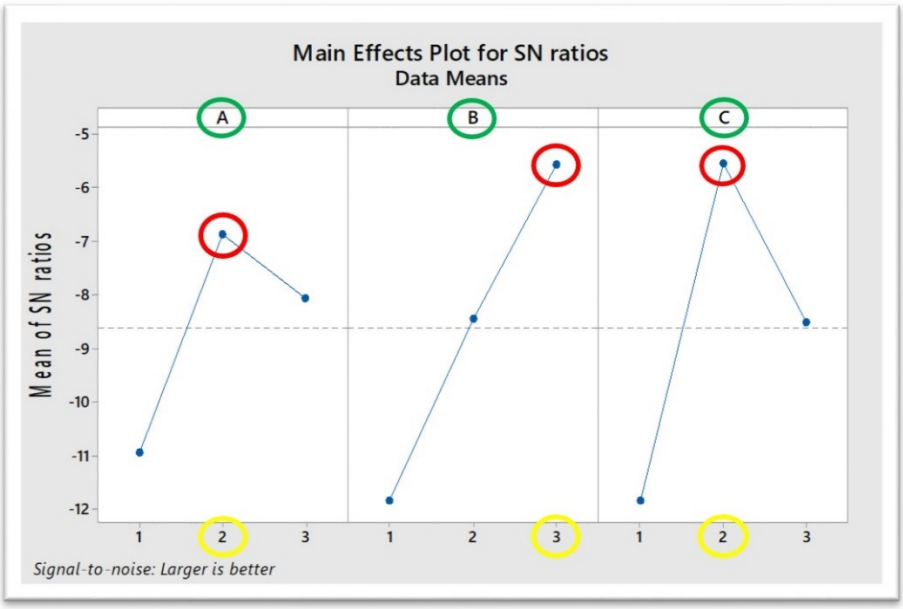

Figure 15: TOPSIS based Taguchi Method "larger is better".

The results obtained from the Minitab software, utilizing the Taguchi method, were integrated into a cohesive outcome through the application of the TOPSIS Method, as detailed in Table 5. The optimal experiment, as determined by this analysis, was performed at a temperature setting of 950°C (A2), with a heat treatment duration of 75 minutes (B3) and employing a quenching process that uses heat treatment oil (C2), as illustrated in Figure 16.

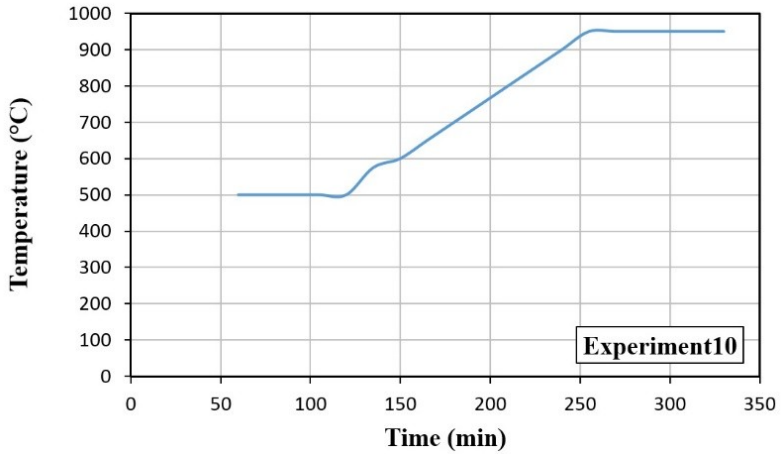

Figure 16: Heat treatment program based on optimization results.

The targeted range for the tensile test is 970-1040 N/mm^2. Upon conducting the tensile test, strength parameters such as elastic modulus, yield value, breaking strength, as well as ductility factors like elongation at break, shrinkage at break, and toughness, were determined. The material's ductility and toughness falling within the specified range affirm the suitability of the temperature, duration time, and quenching media selected during the heat treatment process. Table 6 presents the values for sample number 10, which underwent a 72-hour nitration process at 540 °C.

The impact notch test is conducted to assess the fracture behavior of metals, offering insight into their mechanical properties, particularly under conditions conducive to brittle fracture. As per literature, impact notch tests should yield results of ≥40 J. Table 6 indicates that, based on the experimental design applied, values falling within the "larger is better" criteria range from 154 to 157. Brittle fracture occurs when the sample breaks before undergoing plastic deformation. However, as evidenced by these test results, plastic deformation often occurs before fracture. Under applied force, besides normal (perpendicular) stress, there is an additional shear stress at approximately 45°. Once this shear stress surpasses the material's shear strength (critical shear), elastic deformation transitions into plastic deformation, followed by fracture. This process, known as ductile fracture, results in an uneven and fibrous fracture surface, as depicted in Figure 10. Consequently, the experimental design aligns with literature expectations based on these findings.

The Brinell hardness measurement method involves determining the diameter of an indentation created by applying a specific load over a set period using a hardened ball of known diameter on the material's surface. Results obtained from the experiment fell within the range of 880-1030 N/mm^2, aligning with literature standards. This range ensures that the material maintains an optimal balance: it is neither excessively hard, risking brittleness and breakage, nor too soft, ensuring maximum wear resistance. Consequently, the material's hardness is maintained at an ideal point, delivering the desired outcome in the experiment.

The area under the elongation curve of a material signifies its toughness, which differs significantly between brittle and ductile materials. However, it's crucial to note that this area illustrates the extent of plastic deformation the material can withstand before fracture, rather than strictly representing toughness against sudden impacts and forces.

Table 5: TOPSIS Method application using S/N ratios with weighted application for heat treatment experiments.

Decision Matrix (S/N Ratios)				**Weight Normalized Decision Matrix**				**S_i***	**S_i^-**	**C_i***
Responses	**R_1**	**R_2**	**R_3**		***v_{i1}***	***v_{i2}***	***v_{i3}***			
Weights	**0.333**	**0.333**	**0.333**							
R1	54.11	45.13	31.66	→	**0.13**[b]	0.11	0.09	**0.05**[c]	**0,01**[d]	**0,14**[e]
R2	49.34	45.06	33.29	→	0.12	0.11	0.09	0.05	0,01	0,22
R3	40.59	42.44	50.03	→	0.10	0.11	0.14	0.02	0,06	0,75
R4	47.27	45.13	53.14	→	0.11	0.11	0.15	0.01	0,06	0,83
R5	45.88	43.52	39.93	→	0.11	0.11	0.11	0.03	0,03	0,48
R6	48.21	41.94	33.51	→	0.11	0.11	0.09	0.05	0,01	0,24
R7	50.80	41.90	32.76	→	0.12	0.11	0.09	0.05	0,01	0,15
R8	42.09	43.61	39.93	→	0.10	0.11	0.11	0.03	0,03	0,52
R9	40.13	43.94	41.88	→	0.10	0.11	0.12	0.04	0,19	0,82
-	***140.13***[a]	***130.94***	***120.74***	*A**=	0.11	0.11	0.14	-	-	-
-	-	-	-	A^-=	0.13	0.11	0.09	-	-	-

The expressions a,b,c,d,e indicate sample calculations made in matrices using the relevant equations.

[a] The sum of the squares of each element in the columns

[b] Equation 1→ $v_{1,1}$=0.333*[(54.11/140.13)]=**0.13**

[c] Equation 7→ S_1*={((0.13-0.11+… …+[(0.09-0.14)]}$^{1/2}$=**0.05**

[d] Equation 8 → S_1^-={[(0.13-0.13+… …+[(0.09-0.09)]^2}$^{1/2}$=**0.01**

Equation 9 → C_1*=0.01/(0.01+0.05)=**0.14**

Table 6: Experimental results determined according to Taguchi and TOPSIS methods (sample 10) and determined for comparison (sample 3).

		Required Values					
		Tensile Strength		**Impact Notch**		**Hardness**	
•	**Sample No**	970-1040 N/mm^2		≥ 40 J		970-1040 N/mm^2	
•	**10**	1006	1009	154	151	1030	1028
•	**3**	1049	1035	133	138	1125	1120

The data derived from the Taguchi Method demonstrates an algorithm that enables factors (Factor A, Factor B, and Factor C) to yield an optimal result based on their interdependence. Two explanatory test results reflecting these outcomes as mechanical properties are presented in Table 5. Experiment number 10 aligns with literature standards, providing data that reflects the outcomes obtained by executing the experiment according to the specified factor and level suggested by Taguchi. The performance values of these test conditions in nitration are shown in Table 7.

Table 7: Microvickers test results for Sample 3 and Nitrided Sample 10

Nitriding Process	**Top Surface Hardness ≥ 700 HV**	**Core Hardness ≥ 300 HV**	**Nitriding Depth ≥ 0,1 mm**
Sample 10	870	417	0.10
Sample 3	860	415	0.10

The results from the Microvickers, Tensile Strength, Impact Notch, and Hardness analyses reveal that Sample 10 is the only material that meets all the desired criteria. This result highlights the significance of the study. The production of materials with desired values through the TOPSIS-based Taguchi method has resulted in savings of time, materials, and energy.

4. CONCLUSION

The method emphasizes the relationship between various factors (A, B, and C) to achieve an optimized outcome in terms of mechanical properties, yielding successful results in revealing the connection between the TOPSIS-Based Taguchi Method and factors. The optimization results obtained are significant as the first study in the literature to use the TOPSIS-based Taguchi method. Besides, the results stand out by providing detailed statistical outcomes regarding the optimization of the process conducted with nitriding.

The analysis conducted in the study presents the two most influential test results indicating these outcomes concerning mechanical properties and shows effective results, notably displaying that the trials of Sample 10 are in alignment with the literature standards for mechanical properties.

Sample 5, Sample 8, Sample 9, and Sample 10 are within the targeted tensile strength test range (970-1040 N/mm²), demonstrating satisfactory performance.

Results obtained from the Impact Notch Resistance Test exceeded the expected level (>40 J), indicating a positive performance.

The findings derived from the application of the Taguchi method were systematically synthesized into a coherent outcome utilizing the TOPSIS Method. This statistical analysis identified the conditions for the optimal experiment as a temperature setting of 950 °C, a heat treatment duration of 75 minutes, and the use of oil as the quenching medium. This optimized process led to the successful production of a material characterized by superior performance metrics post-nitration.

In the Hardness Test, Sample 3 and Sample 10 met the specified hardness level (970-1040 N/mm²) and exhibited the desired properties.

The results obtained from the conducted study appear to be better in comparison with the study by Karslı et al. (2021). The surface hardness obtained in the mentioned study is reported as 800 HV and the core hardness at a depth of 0.1 mm is reported as 368 HV. The values obtained with Sample 10, produced through optimization, and Sample 3, selected as a comparison sample, are superior (Table 7).

5. CONFLICT OF INTEREST

The authors declare that there is no conflict of interest.

6. REFERENCES

ARMAD - https://www.aubertduval.com [Accessed 5th June 2022].

Almeida EAD, Costa CE, & Milan JCG. Study of the nitrided layer obtained by different nitriding methods. Matéria (Rio de Janeiro). 2015:20(2): 465.

Bakdemir SA, Özkan D, Türküz MC, Uzun E, & Salman S. Effect of the nitriding process in the wear behaviour of DIN 1.2344 hot work steel. Journal of Naval Sciences and Engineering. 2020:16(1): 45-70.

Callister WD & Rethwisch DG. Materials Science and Engineering: An Introduction, 8th ed.: John Wiley & Sons; 2009.

Cengiz M. Hardox 400 Çelik Yüzeyinin Plazma Transferli Ark Kaynak Yöntemiyle Alaşımlandırılması ve Taguchi Metoduyla Değerlendirilmesi. Dicle University Journal of Engineering (DUJE). 2019:10(3): 969-979.

Du H, Somers MAJ, & Agren J. Microstructural and compositional Evolution of Compound Layers during Gaseous Nitrocarburizing. Metallurgical and Materials Transactions A: Physical Metallurgy and Materials Science. 2000:31A: 195-211.

Canıyılmaz E, & Kutay F. Taguchı Metodunda Varyans Analizine Alternatif Bir Yaklaşım. Gazi Üniversitesi Mühendislik Mimarlık Fakültesi Dergisi. 2003:18(3): 51–63.

Ferreira L, Brunatto SF, & Cardoso RP. Martensitic Stainless Steels Low Temperature Nitriding: Dependence of Substrate Composition. Materials research. 2015:18: 622-627.

Friehling PB, & Somers MAJ. Growth Kinetics of the Compound Layer on Gaseous Nitriding of Iron: The Effect of the Surface Reaction in Mass and Carge Transport in Inorganic Devices: Fundamentals to Devices (Part B). Techna Srl; 2000.

GÖKSU (2015). Web site. https://www.otuken.com.tr. [Accessed 3th January 2022]

Gür AK & Kaya S. Abrasive Wear Resistance Optimization of Three Different Carbide Coatings by The Taguchi Method. Mater. Test. 2017:595: 450–455.

HASCOMETAL - http://www.hascometal.com/teknik-bilgiler.aspx?ID=68 [Accessed 1st October 2021]

HASÇELİK - https://hascelik.com/celik-hakkinda-genel-bilgiler/celik-nedir [Accessed 1st May 2022]

Haefer R & Ilschner B. Oberflachen- und Dünnschicht-Technologie. Springer Verlag; 1991.

Hwang CL & Yoon P. Multiple Attribute Decision Making In: Lecture Notes In Economics And Mathematical Systems. Springer Verlag; 1981.

Joseph, R. Heat Treatments of Steels, 10th edition, ASM.: 91. 465 pages, American Society for Metals; 1973.

Karslı M, Kemikoğlu U & Yavuz S. Tabanca Namlu Malzemesi 32CrMoV12-10 Alaşımına Uygulanan Gaz Nitrasyon ve Su Verme İşlemlerinin Darbe Dayanımına Etkisinin İncelenmesi. Gümüşhane University Journal of Science and Technology, 2021:11(4), 1198-1207.

Kaya S. Yüzeyi Modifiye Edilmiş Ferritik Paslanmaz Çeliğin Aşınma Direncinin Taguchi Metoduyla Optimizasyonu. Master Thesis, Fırat University, Graduate School of Natural and Applied Sciences, 105 pages, Elazığ; 2017.

Phadke M. Quality Engineering Using Robust Design Book, Library of Congress Catologing AT & T Bell Laboratories, New Jersey, USA; 1989.

Şirvancı M. Kalite için deney tasarımı, Taguchi Yaklaşımı. Literatür Publications, 112 pages, İstanbul; 2011.

Özay Ç. Teğetsel tornalama-frezeleme yönteminde işleme parametrelerinin teorik ve deneysel olarak araştırılması. PhD Thesis, Fırat University, Graduate School of Natural and Applied Sciences, Elazığ; 2009.

Ross PJ. Taguchi Techniques for Quality Engineering, Loss Fuction, Orthogonal Exp. Param. Toler. Des., 279 pages., Mcgraw-Hill; 1998.

Rutci AT. Development of Barrel Material Used in Light Weapons and Investigations of Manufacturing Process Parameters. Master Thesis, Sakarya University, Institute of Natural Sciences, Sakarya; 2019.

Saklakoğlu N, Gençalp İrizalp S, İldaş G & Demirok S. Microstructure and wear properties of Fe-based hardfacing alloy / Fe esaslı sert kaplama alaşımının mikroyapı ve aşınma özelliklerinin incelenmesi. Celal Bayar University Journal of Science. 2016:12(3): 517-523.

SIJ GROUP - https://www.sij.si/en/sij-brands/sinoxx/ [Accessed 1st October 2021].

Şimşek B. Hazır Betonun Optimal Karışım Oranlarının Belirlenmesi İçin Bir Çok Yanıtlı Modelleme ve En İyileme Uygulaması: Topsis Tabanlı Taguchi Yaklaşımı İle Cevap Yüzey Yöntemi. PhD Thesis, Ankara University, Graduate School of Natural and Applied Sciences, Ankara; 2014.

Tekin A. Çelik ve Isıl İşlemi Bofors El Kitabı. Hakan Ofset Publications, 616 pages, İstanbul; 1984.

Toktaş G & Toktaş A & Duran, M. Investigating The Wear Behaviour of Induction Hardened 100Cr6 Steel. Sakarya University Journal of Science. 2018:225:1174-1180.

Topbaş AM. Çelik ve Isıl İşlem El Kitabı. Ekim Ofset Publications, 553 pages, İstanbul; 1998.

Uzkut M & Özdemir İ. Farklı Çeliklere Uygulanan Değişen Isıtma Hızlarının Mekanik Özelliklere Etkisinin İncelenmesi. Dokuz Eylül Üniversitesi Mühendislik

Fakültesi Fen Ve Mühendislik Dergisi, c. 2001:3(3): 65-73.

Yang M. Nitriding- Fundamentals, modeling and process optimization. PhD Thesis, Worcester Polytechnic University, Material Science and Engineering, Worchester/USA; 2012.

Weststrate CJ. Hydrocarbon and Ammonia Chemistry on Noble Metal Surfaces. PhD Thesis, Leiden Universty Leiden Institute of Chemistry LIC, Faculty of Science, Leiden/Holland; 2006.